Available online at www.sciencedirect.com
ScienceDirect
Aerospace Science and Technology 12 (2008) 515–523
Aerospace Science and Technology
www.elsevier.com/locate/aescte

Preliminary study to raise axial flow compressors up to the context-awareness standards

Babak Aryana [1]

Aerospace Engineering-Propulsion Systems, Baghehoze Street, Shiraz, Iran

Received 18 August 2006; received in revised form 15 November 2007; accepted 21 December 2007

Available online 15 January 2008

Abstract

This paper explains summary of a method to introduce context-awareness into gas turbine engines, which urges making essential changes in power transmission and compression process. Applying these changes on axial flow compressors enhances individual and free access to each component, and then conventional methods to design and model their characteristic map should be adapted aptly. Accordingly, suitable methodology is introduced, and based on that, an alternative to HPC of GE90-94B turbofan engine is designed and modeled by computer in average-fidelity level.

Keywords: Context-awareness; Gas turbine; Axial flow compressor; Computer modeling; Design method; Characteristic map

1. Introduction

Direct interaction of computer and IT technology with human has developed the concept of context-awareness since early 1990s. In fact, an article posed this concept, which discussed the idea of orienting computer productions with different aspects of people behaviors [7]. Currently context-awareness has a broad and profound meaning, which appears in the cyberspace; in this global network, high ability for adapting to user demands and different environmental elements is the crucial character without it this huge system is paralysis. In a word, context-awareness can be defined as adaptation ability to user demands and environmental elements.

Although entity of gas turbine engines completely differs from computers, however, potential of these engines to utilize context-awareness is considerable. This fact that different operators use theses systems in different environments shows this strong potential.

The key to raise a device up to context-aware system is to create capability of free and individual access to all effective components to tune their operations toward environmental elements and user demands. This specification obviously is seen in structure of computer technology, which allows executive software to access freely and individually to all influential components from user opinion to effective hardware parts.

In the contrary, conventional architecture of gas turbine engines creates limit area to access to components individually. Major sections of these engines are linked so strongly that individual access to their components particularly in compressor is less than that should be.

To heighten access ability, coherent consistency should replace this strong link; consequently, all effective components of all sections are capable to tune toward environmental elements and user demands independently and consistently.

As a result, approaching gas turbine engine to desirable characters requires making essential changes in power transmission and compressor configuration. Two major ways appear for this work: one designing new generation of compressors capable to satisfy context-awareness requirements and the other changing available types to near them to proper devices.

Author believes adjusting conventional compressors toward desirable specifications is possible. The best way to make such changes is to use electric energy in the basis of new technologies, which create light and compact electric rotary machines capable to fit into a stage disk. Two significant technologies

E-mail address: Babak.Aryana@Gmail.com.
[1] Independent researcher.

1270-9638/$ – see front matter
doi:10.1016/j.ast.2007.12.004

Nomenclature

C	air velocity – also – coefficient
c	chord
IR	increment of hub-tip ratio stage by stage
i	incidence angle
K	coefficient to determine taper of blades
m	air mass flow rate
N	rotational speed
P	pressure
R	radius ratio
r	blades radius
s	blades pitch or space
T	temperature
U	rotor blades velocity
V	air relative velocity to blade
α	angle between air approaching velocity and axial velocity
β	angle between air relative velocity and axial velocity
δ	angle between air vector mean velocity and air axial velocity
η	efficiency
Λ	degree of reaction
$\Delta\theta$	air turning angle
θ	blades camber angle
ρ	density
σ	centrifugal stress
ζ	cascade stagger angle

Abbreviations

CNT	Carbon Nano Tubes
EEE	Energy Efficient Engine
GE	General Electric Company
HPC	High Pressure Compressor
HTS	High Temperature Superconductor
IT	Information Technology
SSL	Standard Sea Level

Units

kg	kilogram
m	meter
s	second

Suffix

0	stagnation state
1	inlet to compressor – also – inlet to rotor
2	inlet to combustor – also – exit from rotor
3	exit from stator
a	axial
b	blades
C	compressor
ct	critical
D	total drag
i	stage number
m	mean radius
R	relative to design value
r	root radius – also – radial component
S	stage
t	tip radius
w	whirl component

promise producing such an electrical machine, one High Temperature Superconductors (HTS), which are currently being implemented to design particularly compact and lightweight rotary machines [6], and the other Carbon Nano Tubes (CNT) whose different potentials such as very little and light electric motors are under development [3].

However, theses changes impose new complexities digesting those is hard for conservative world of gas turbine engines. On the other hand, new technologies are able to help designing more efficient and suitable compressors inherently capable to adapt to context-awareness standards [1].

Nevertheless, a preliminary study of methodology to apply context-awareness on conventional compressors and its effects on their operations can indicate the values of this work.

This article explains summary of a study to apply such a mechanism on axial flow compressors. In this study, it is assumed that compressor's stages are able to receive needful energy individually and convert that independently, and thus they are capable to adapt themselves to environmental elements and user demands by changing rotational speed.

2. Recognition of environmental elements and user demands

To apply context-awareness, first step is to identify and measure environmental elements and user demands. Environmental elements for an axial flow compressor are the parameters forming its working condition and defining its limitations. Therefore, they can be defined as the parameters moving each compressor stage into surge margin. Besides, individual rotational speed for each stage inherently makes optimum rotational speed rise stage by stage, which needs to add structural limitation to other limitations.

User demands are considered parameters mingled with the off-design condition and imposed on the stages along with environmental elements.

To evaluate the concept, author developed exclusive software capable to design and model context-aware gas turbine engine in average-fidelity level. Accordingly, methods for preliminary design of axial flow compressors were adapted to requirements.

2.1. Methodology to measure flow separation

In this study, to determine flow condition in the all regions, methods explained in the [2] were used and adjusted to the problem.

2.1.1. Subsonic regions

In this region for assessing flow condition, [2] suggests an experimental method in which stagnation pressure loss is used as indicator. Cascades specifications such as their incidence angles and air deflections are effective parameters in this measurement (more details can be found in [2] or similar textbooks).

In the current work, a proper method was derived to use in computer programming; accordingly, the best fit for empirical graph, suggested by [2] for total head loss variation versus deflection angle, were found by *Mathematica* software [11]; afterwards, resulted equations were used to determine mean total head loss by regard to air deflection angle. Using these graphs, suitable cascades incidence angle also can be calculated.

2.1.2. Supersonic/transonic regions

[2] suggests a shock model for double circular arc blades in which blades pitch defines shock condition there. In fact, these spaces determine angles by which supersonic flow turns to suction surface of blades where the flow is tangent to the surface: the less space (increasing solidity), the lower shock loss. In this condition, as flow enters to passage between two blades, its velocity is increased due to expansion compatible with Prandtl–Mayer relation [10], then in the passage entrance at point B (Fig. 1) a bow shock is created whose extension is extended to front of leading edge of neighboring blade at point C. This assumption is reasonable that loss across the shock can be estimated by the normal shock loss taken for the average Mach numbers at point A and B. Mach number at A is inlet relative Mach number and Mach number at B is a function of this inlet Mach number and flow supersonic turning angle to point B. The empirical graphs suggested by [2] for measuring shock loss, need to find flow-turning angle $\Delta\theta$ first Fig. 1 (more details can be found in [2] and other similar textbooks).

In order to obtain acceptable estimation for $\Delta\theta$, author considered two simplifications:

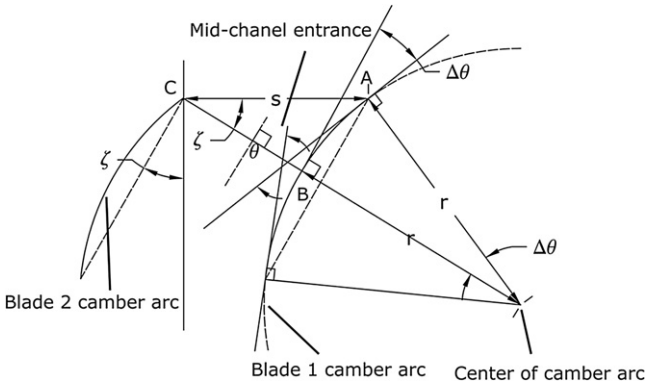

Fig. 1. Shock model.

– Firstly, instead of lower and upper surfaces of cascades, camber arcs of their airfoils are taken as flow and cascades interaction plane. This assumption is acceptable, because thin airfoils are used for transonic cascades.
– Secondly, airfoils camber arcs are considered circular, which is reasonable assumption, because tolerable shock losses arise in the little $\Delta\theta$ resulting in acceptable outcomes for other form camber arcs.

As Fig. 1 indicates, length of base of right-angled triangle CBA approaches length of arc AB if value of pitch approaches zero. Therefore, for little $\Delta\theta$ (less than 2 degree) in which shock loss is bearable, following equation yields acceptable estimation for turning angle:

$$\Delta\theta \approx \frac{\sin(\zeta)\cdot s}{r} + i \tag{1}$$

Similar to subsonic state, the best fits for graphs, suggested by [2] to estimate shock loss, were obtained by *Mathematica*, then their equations were used in computer program in order to measure flow condition at intended locations. Eq. (1) has also been used to estimate $\Delta\theta$ by regard to cascades specifications.

2.2. Methodology to estimate structural limitations

Centrifugal stress at rotor blades roots influences stage pressure ratio. This factor is a function of rotor rotational speed, and thus crucial in this study.

[2] suggests following equation to measure critical centrifugal stress:

$$(\sigma_{ct})_{max} = \frac{\rho_b}{2} U_t^2 \left[1 - \left(\frac{r_r}{r_t}\right)^2\right] K \tag{2}$$

In this step, to gain more general results any specific material was not selected for rotor blades and their materials were considered uniform in all stages, and hence, any specific value could not be defined for maximum allowable critical centrifugal stress.

Accordingly, author took ratio of critical centrifugal stress per blades density to define maximum allowable rotor rotational speed. Obviously, stage having minimum hub-tip ratio suffers maximum critical centrifugal stress, namely, first stage; thereby for a given rotational speed, this ratio has maximum allowable value in this stage:

$$\frac{(\sigma_{ct})_{max}}{\rho_b} = \frac{U_t^2}{2}\left[1 - \left(\frac{r_r}{r_t}\right)^2\right] K \tag{3}$$

In the computer programming, author used Eq. (3) to obtain an index for maximum allowable $(\sigma_{ct})_{max}/\rho_b$. In this way, this ratio is calculated by a safe rotational speed given by designer and hub-tip ratio of first stage, whose result is saved as the index. During design process, $(\sigma_{ct})_{max}/\rho_b$ is calculated for each stage and ratio of that per that of first stage is measured, therefore allowable value of this ratio for each stage must be between 0 and 1. Clearly, by increasing hub-tip ratio maximum allowable rotational speed can increase stage by stage.

3. Methodology of designing and modeling

Particular design method in this study should support selecting optimum rotational speed for each stage individually, which affects calculations and procedures.

3.1. Design

To start design process, designer should define some compressor specifications:

A. First stage's hub-tip ratio.
B. Value of increment of hub-tip ratio stage by stage (IR).
C. The safe blades tip speed for first stage to determine maximum allowable ratio of Eq. (3).
D. Blading type, to determine velocities distribution along the blades.
E. Annulus shape to form blading.

In the average-fidelity level analysis, velocities along the rotors and stators blades are considered three dimensional, similar to method used by [2] in which whirl velocities and degree of reactions are defined as follow:

$$C_{w1} = aR^n - \frac{b}{R} \quad \text{and} \quad C_{w2} = aR^n + \frac{b}{R} \tag{4}$$

where "n", "a" and "b" are constant and "R" is the radius ratio r/r_{mort}. Degree of reaction can be written as

$$\Lambda = 1 - \frac{C_{w2} + C_{w1}}{U} \tag{5}$$

and the blades speed is given by

$$U = U_{mort} R \tag{6}$$

immediately seen that

$$(C_{w2} - C_{w1}) = 2b/R \tag{7}$$

By taking three values for "n" three types for velocities and distribution of degree of reactions (bladings) are obtained. More details of this analysis can be seen in [2] and similar textbooks.

In this study, for defining annulus shape two major types were selected:

1. Constant outer diameter in which C_{at} = constant and $U_{t1} = U_{t2}$.
2. Constant mean diameter in which C_{am} = constant and $U_{m1} = U_{m2}$.

Defining annulus shape is precondition to determine velocities' triangles. Usually three main radii are taken to calculate these triangles, namely root, mean and tip. Method and formulation to calculate these triangles can be found in the [2,4] or other similar textbooks.

At the first point of designing each stage, designer should determine following characteristics [2]:

1. Degree of reaction (at mean or tip radius, depending on annulus shape).
2. Stage temperature rise.
3. Blades aspect ratio.
4. Blades tapered coefficient (K).
5. Ratio of the point of maximum camber.

These characteristics are used to calculate geometrical and aerothermodynamic specifications in the three major aforementioned radii; however, they relatively change during calculations.

Besides major radii, all stages' specifications are calculated at two major locations: at entrance and exit of rotor. For instance in constant-outer-diameter design, root and mean radii at rotors' entrance differ from that of their exit. Following relation is set to calculate r_r at entrance:

$$r_{r1} = (r_r/r_t) r_t \tag{8}$$

Therefore, r_r at rotors' exit is:

$$r_{r2} = r_t(\mathrm{IR}/2 + r_r/r_t) \tag{9}$$

Compatible with root radii, mean radii are:

$$r_{m2} = (r_{r2} + r_t)/2 \tag{10}$$

In constant-mean-diameter design, mean radius is considered constant and similar process is carried out to obtain root and tip radii.

Aforementioned specifications open the door to calculate more sophisticated characteristic of the stage. Absolute performance of the stage is taken at mean radius, but all characteristics are calculated at three major radii.

Following characteristics are calculated orderly to determine more accurate stage performance [2]:

1. *Velocities triangles*. By regard to this fact that defining the best specifications for the best performance is a principle to design cascades, in order to determine inlet angles to rotors, deflection angles of the stators are considered for generating minimum possible stagnation pressure loss. Accordingly, the software sets the stator deflection ($\alpha_2 - \alpha_3$) to 30 degree in all stages but first stage (see Fig. 5).
2. *Stage rotational speed*. To set this speed, structural limitation is the first criteria checked according to method explained in Section 3.2.
3. *Mach number at rotors' tip and stators' hub*. According to method explained in Section 2.1.2, if flow Mach number indicates high risk of separation necessity of redesign is warned to designer. In addition, this parameter restricts rotational speed.
4. *Stagnation pressure loss*. Overall stagnation pressure loss is calculated as follow: *Overall Loss* = $\Lambda \times$ *Rotor Loss* + $(1 - \Lambda) \times$ *Stator Loss*. Designer is able to set the loss in the acceptable range when software indicates its value. This parameter, which is third factor to restrict rotational speed, is measured at mean radius.
5. *Stage temperature rise* (*stagnation and static*). This specification is recalculated according to more precise characteristic of stage obtained up to now.

6. *Rotor and stator blades pitch/chord ratio, pitch, chord and number of those*. In order to clear geometrical specification of stage, incidence, stagger, camber, deviation, inlet and outlet angles are calculated. Sources of theses calculations are velocities' triangles solved by software and geometrical specification defined by designer.
7. *Lift and drag coefficients*. Tree major drag coefficients are considered in this study: profile drag, secondary loss and annulus drag, whose summation determines total drag coefficient.
8. *Efficiency of the blades row* (η_b).
9. *Stage efficiency*.
10. *Stage stagnation and static pressure ratios*.

3.2. Modeling compressor operation

In this study, showing capability of the system to face any operating condition is the most crucial aim. Therefore, compressor modeling was selected to impose arbitrary off-design condition on the compressor components and model their behaviors. Arbitrary off-design condition defines new environmental elements causing specific performance in the compressor, which is known as its behavior. Specifications defined during design process and saved as data identify each component.

3.2.1. Identifying design

Design contains overall characteristic of compressor predefined by designer in the design start point, dimensional characteristic of stages and item 6 in the orderly design of stage explained in Section 3.1.

Other items of orderly design process are also followed here to calculate aerothermodynamic characteristic of stages. However, to calculate air exit angle of each stage's stator, method used in design process is not functional (item 1). In fact, cascades' specifications have already determined in the design and they must remain same in the off-design conditions. In this case, the point mentioned by [5] was considered. This reference's cascades data has suggested that air exit angles, namely β_2 for rotor and α_3 for stator do not change appreciably for a range of incidence up to the stall point. By some simplifications, for a given stage it can be inferred that:

$$\tan\alpha_3 + \tan\beta_2 = \text{constant} \tag{11}$$

It is assumed that Eq. (11) governs flow around the stators before the stall bounds. Thereby its values could be calculated and recorded during design process for all stages, and then α_3 of each stage in the arbitrary off-design conditions can be estimated by using recorded value of Eq. (11) and β_2 of previous stage.

Because of individual speed in each stage, this assumption can be implemented reasonably. This specification allows preventing flow separation, so that stage would be kept outside the stall margin.

3.2.2. Modeling the design operation

Conventionally, rotational speed has been used to categorize compressors characteristic maps. However, using this speed to illustrate overall performance of intended type is obviously insignificant.

Clearly, particular bound for this type should indicate the limit beyond that changing rotational speed could not help flow separation. Intended type of compressor's stages may confront with flow separation when $\alpha_1 + \beta_1$ overruns specific limits and then inlet axial velocity has crucial role to lead stages into surge margin.

As a result, new dimensionless parameter $\frac{C_a}{\sqrt{T_1}}\big|_R$ which represents effects of this key parameter, was defined by author to analyze compressor characteristic. Nevertheless, author considered summation of stages rotational speed per square root of its inlet stagnation temperature relative to design value, namely $\sum(\frac{N_i}{\sqrt{T_{0i}}})_R$, to show effects of stages rotational speeds on off-design operations. To facilitate assortment of results, effect of rotational speed regulation on this ratio is ignored.

Exclusive software developed for this study uses two ways to form off-design condition. One by defining a point by new air inlet axial velocity, rotational speed and altitude based on percentage of their design value, and the other by defining an off-design condition envelope formed by changing altitudes, $\frac{C_a}{\sqrt{T_1}}\big|_R$ and $\sum(\frac{N_i}{\sqrt{T_{0i}}})_R$ in a wide range. In all methods, each point is imposed on the compressor from first stages singly.

When new environmental elements formed by off-design condition moves each compressor stage into surge margin, the software attempts to exit stage from this by changing its rotational speed; if it cannot return stage to safe situation this off-design condition is not classified as a point of compressor working envelop. The points detected as members of compressor working envelope form its characteristic map together. Mechanism to regulate rotational speed is tabulated in Table 2. Note deflection is $\alpha_2 - \alpha_3$ for stator and $\beta_1 - \beta_2$ for rotor Fig. 5.

4. Alternative design of GE90-94B HPC

GE90-94B is a high by pass ratio turbofan engine powering Boeing 777-300ER. High-pressure compressor of this engine has 10 stages and its pressure ratio at design point is 1:23 for 55 kg/s airflow (Fig. 2).

To demonstrate distinctions between intended type of axial flow compressor and conventional type, this engine's HPC was designed alternatively and then its characteristic map was drawn.

In order to form the compressor, hub-tip ratio of first stage was set to 0.5, IR was selected equal to 0.05, the safe blades tip speed was set to 360 m/s (Eq. (3)), blading type was selected exponential and finally constant outer diameter selected for annulus shape. Acceptable limit for stagnation pressure loss was also set to 0.037 (generated by deflection limits in Table 2) and for shock loss to 0.005. These specifications are common selections for preliminary design of transonic axial flow compressors [2]. In addition, the GE Energy Efficient Engine (EEE) high-pressure compressor map was used for qualitative comparison (see [9]) Fig. 3.

To draw compressor characteristic map, altitude was varied from 0 to 20000 meters by increment of 500, $\frac{C_a}{\sqrt{T_1}}\big|_R$ was varied

from 0.3 to 1.1 by increment of 0.01 and $\sum(\frac{N_i}{\sqrt{T_{0i}}})_R$ was varied from 0.1 to 1.1 by increment of 0.01.

Two major types of graphs were drawn; one shows variation of stagnation pressure ratio and efficiency versus $\frac{m\sqrt{T_{01}}}{P_{01}}\big|_R$ for different values of $\frac{C_a}{\sqrt{T_1}}\big|_R$ Fig. 7, and the other shows such dimensionless parameters versus correct airflow for different values of $\sum(\frac{N_i}{\sqrt{T_{0i}}})_R$ Fig. 6.

5. Results

The software uses methodology explained in Sections 2 through 4 to design alternative compressor and model its behavior. Summary of outcomes is as follow.

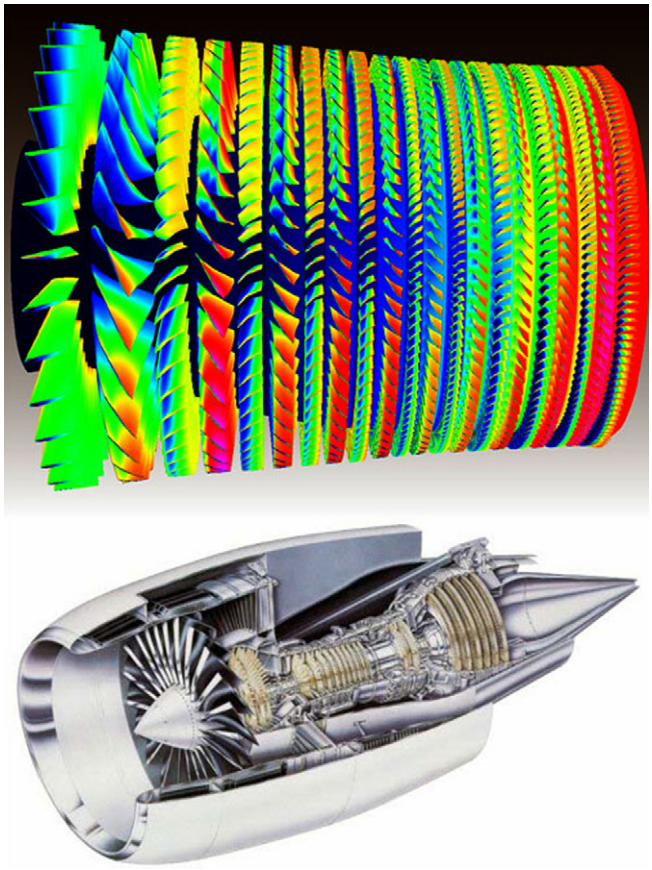

Fig. 2. GE90 turbofan engine and its HPC.

5.1. Design

Two important characteristics are seen in the results of design, which are higher efficiency and pressure ratio (see Table 1). These specifications are direct result of optimum and maximum rotational speed in the stages.

As it was explained in Section 3.1, three parameters are considered for setting speed of each stage. One is stagnation pressure loss, another is shock loss and the other is critical cen-

Table 2
Method to regulate rotor rotational speed

Flow status ↓ Regulation status →	Rotational speed is increased	Rotational speed is decreased
Deflection angle at rotor or stator mean radius $\geqslant 38°$	⊗	
Deflection angle at rotor or stator mean radius $\leqslant 12°$		⊗
Shock loss at rotor tip or stator hub < 0 (out of available curve)	⊗	
Shock loss at rotor tip or stator hub $\geqslant 0.005$		⊗

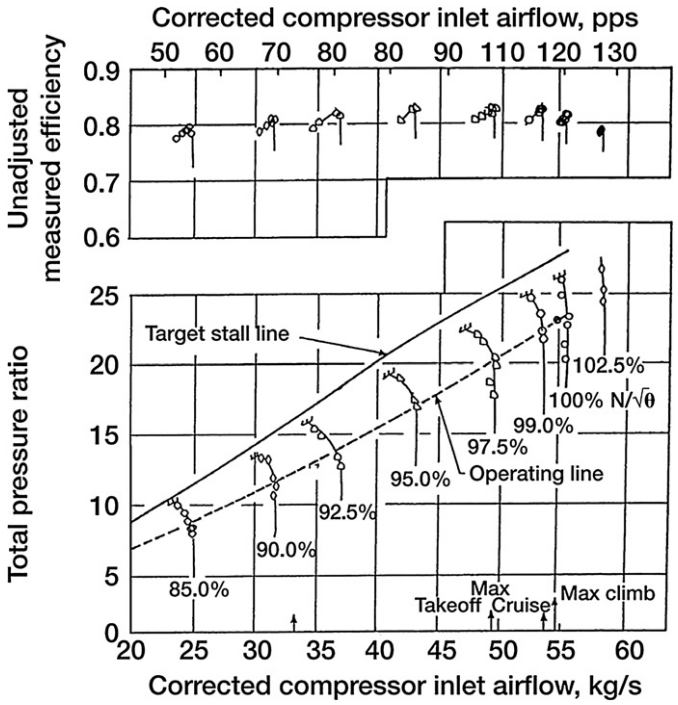

Fig. 3. Energy Efficient Engine (EEE) high-pressure compressor map of GE90-94B turbofan engine (see Ref. [8] for similar map).

Table 1
Some characteristic of alternative compressor stages

Stage no.	Rotational speed [rev./s]	Temperature rise [Kelvin]	Pressure ratio	Efficiency	Rotor tip Mach number	Stator hub Mach number	$(\sigma_{ct})_{max}/\rho_b$ per index
1	151.574	44.7953	1.57429	0.925269	1.1	0.626387	–
2	165.005	49.9912	1.56215	0.935832	1.07679	0.666505	1
3	172.258	56.5019	1.5579	0.942098	1.0343	0.621095	1
4	181.34	64.2407	1.56172	0.952951	1.00121	0.58106	1
5	192.967	72.0808	1.55534	0.960881	0.979721	0.545488	1
6	208.343	82.015	1.55858	0.967534	0.975031	0.517258	1
7	229.677	96.7388	1.5857	0.973661	0.993031	0.49889	1

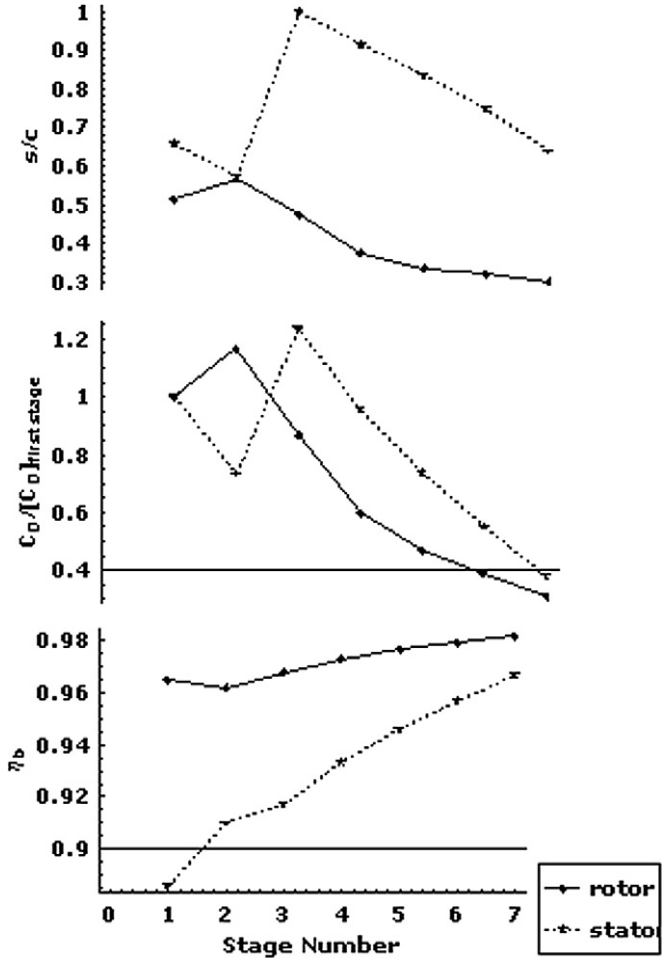

Fig. 4. Stage-by-stage changes of parameters effective on stage efficiency.

trifugal stress. By regard to these parameters, stage-by-stage increases of temperature and hub-tip ratio allow increase of speed stage by stage. Rise of temperature delays compressibility effects and higher hub-tip ratio increases allowable critical centrifugal stress, which permit rotating by higher speed.

Increase of rotational speed expectedly widens velocities triangles, which raises differences between whirl components at entrances and exits of rotors Fig. 5. Increase of air outlet angle decreases pitch chord ratio (s/c), which increases blades number and decreases total drag coefficient. Such a situation makes also vector mean velocity closes in on the air axial velocity (reduction of δ), which raises blades row lift coefficient and decreases its drag coefficient. Total result of these changes is higher blades row efficiency (η_b) defined as the ratio of the actual pressure rise to the theoretical pressure rise. Therefore, pressure loss affects this ratio directly and maintaining that into acceptable range additionally influences blades row efficiency Fig. 4.

Stage efficiency is related to blades row efficiency by following relation: $\eta_S = \Lambda\eta_{b(rotor)} + (1-\Lambda)\eta_{b(stator)}$ [2], and then, result of its rise would be increase of stage efficiency.

On the other hand, higher difference between whirl velocities increases work done by stage. This higher work done is also boosted by higher stage efficiency, and finally the more work done the higher stage pressure ratio.

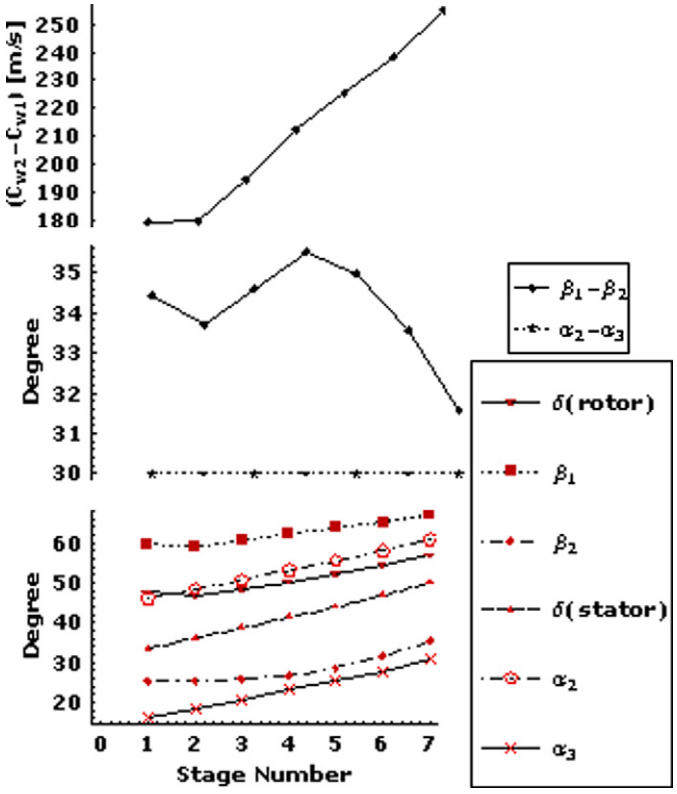

Fig. 5. Air angles, deflections and whirl velocities variations through the stages.

By regard to Table 1, this is clear that except first stage, in which exceed shock loss restricts rotational speed, critical centrifugal stress limits other stages' speeds (ratio per index = 1). This situation influences variation of δ and β (Fig. 5) whose effects appear in rotors' pitch chord ratios, drag coefficients and η_b (Fig. 4). Rotors' air angles increase after a decrease between stages 1 and 2, and then reverse reaction expectedly is seen in their s/c and drags, whose effect is a reaction similar to the rotors' angles for their η_b. Stator specifications, but, experience slightly different situations. During design process, $\alpha_2 - \alpha_3$ is kept equal to 30 degree (Fig. 4), which causes steady increase of stator air angles Fig. 5. Interaction of this different behavior with rotors' air angles causes surge of stators' s/c from stages 1 to 3 whose effect appears in drag. However, influential parameters of rotors and stators generally change toward increase of stages efficiency and pressure ratio.

Although effects of optimum rotational speed in the stages already have been known, nevertheless effects of dynamic regulation compatible with environmental elements have not been considered so far. As the results show, setting optimum rotational speeds in the stages dramatically affects stages performance whose first effect is reduction of stages number for given pressure ratio: 7 stages beside 10 stages for pressure ratio 1:23 and 50 kg/s airflow at static condition in SSL.

5.2. *Off-design*

As it was discussed, performance of stage is strongly linked to its rotational speed, and then each stage operation could be handled by regulating its speed. This specification shows its

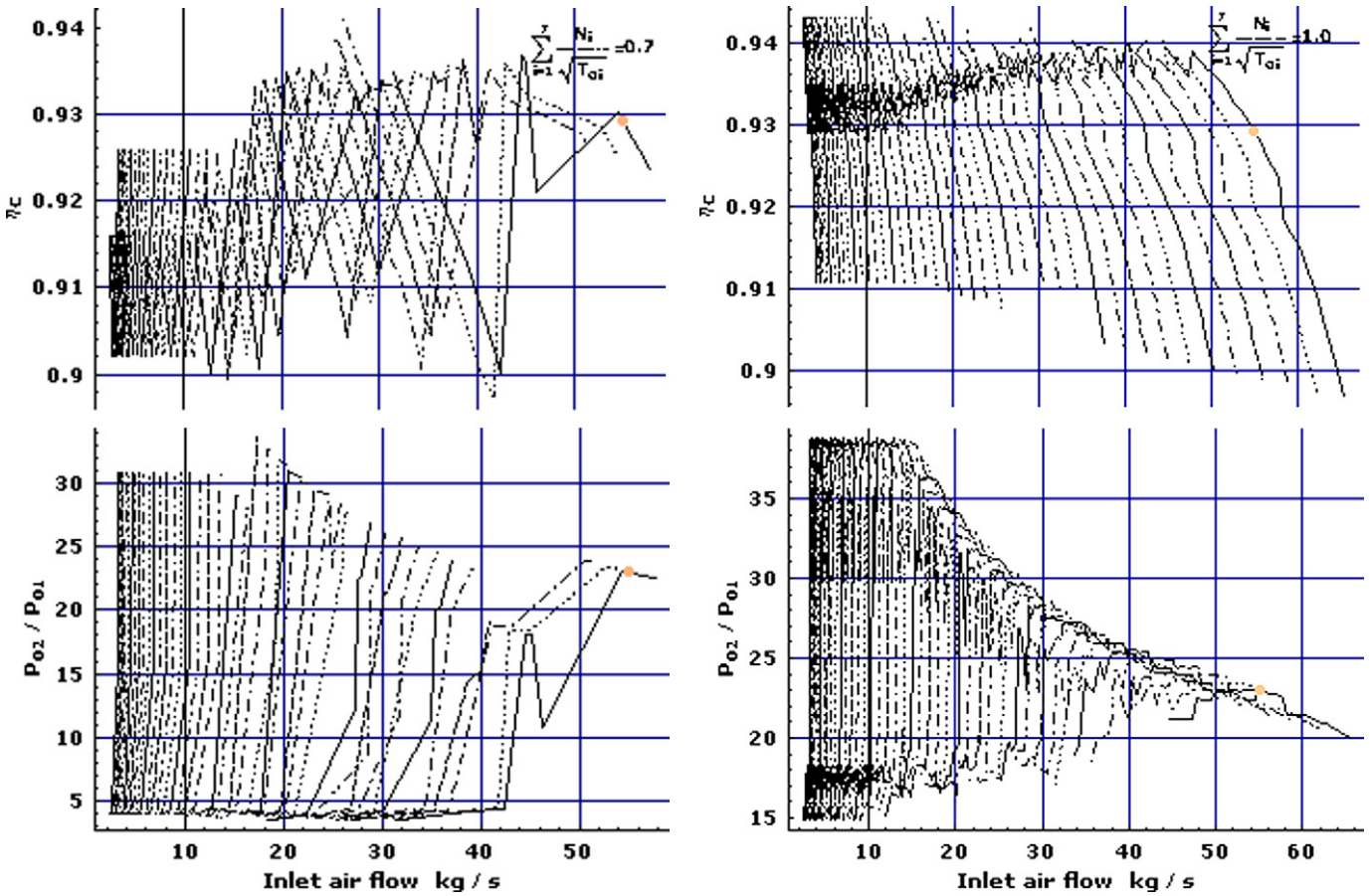

(a) (b)

Fig. 6. Characteristic maps of alternative compressor for different values of $\sum(\frac{N_i}{\sqrt{T_{0i}}})$ (relative to design value).

Table 3
Rotational speed regulation prevents stall in the stages

	Pressure loss at rotor mean	Deflection angle at rotor mean [degree]	Rotor tip Mach number	Shock loss coefficient	$(\sigma_{ct})_{max}/\rho_b$ per index	Rotational speed [rev/s]
Stage 2 *Before* regulation	0.0195	34.8	1.14	**0.079**	1.0	140
Stage 2 *After* regulation	0.03	37.3	0.909	*0.0*	0.603	128
Stage 4 *Before* regulation	**0.129**	36.2	1.09	0.0	1.0	154
Stage 4 *After* regulation	*0.02*	35.9	1.02	0.0	0.68	149

own important effect at off-design operation of compressor. For example following off-design condition is applied on the compressor:

1. Altitude 10000 meters.
2. Inlet axial velocity 85% of design value.
3. Rotors rotational speed 85% of design value.

Rotor blades tips in stage 2 confront with extreme shock loss and deflection angles at means of rotor blades in stage 4 produce high stagnation pressure loss. Regulation of rotational speed solves these problems. Outlines of stages performances and system reactions are indicated in the Table 3. Note stages are fallen into new condition singly from first to end and when a stage confronts unacceptable situation, firstly, its situation is improved by speed regulation then its outlet is applied on the next stage.

The software similarly uses such a system to apply an off-design condition envelope on design and model its behavior. Although individual rotational speed of each stage compels using different method to draw this type of compressor's characteristic maps, yet effects of adaptation ability to environmental elements and user demands are clear (compare Figs. 3 and 6). Working envelope of compressor for $\sum(\frac{N_i}{\sqrt{T_{0i}}})_R \geqslant 0.5$ encompasses an area rather a line Fig. 6.

However, real working envelope of this type of compressor can be indicated by maps drawn on the basis of $\frac{C_a}{\sqrt{T_1}}\big|_R$. Characteristic map drawn for this dimensionless parameter shows that for $\frac{C_a}{\sqrt{T_1}}\big|_R > 0.5$ compressor is capable to deliver relatively wide range of pressure ratio when input condition (airflow, stag-

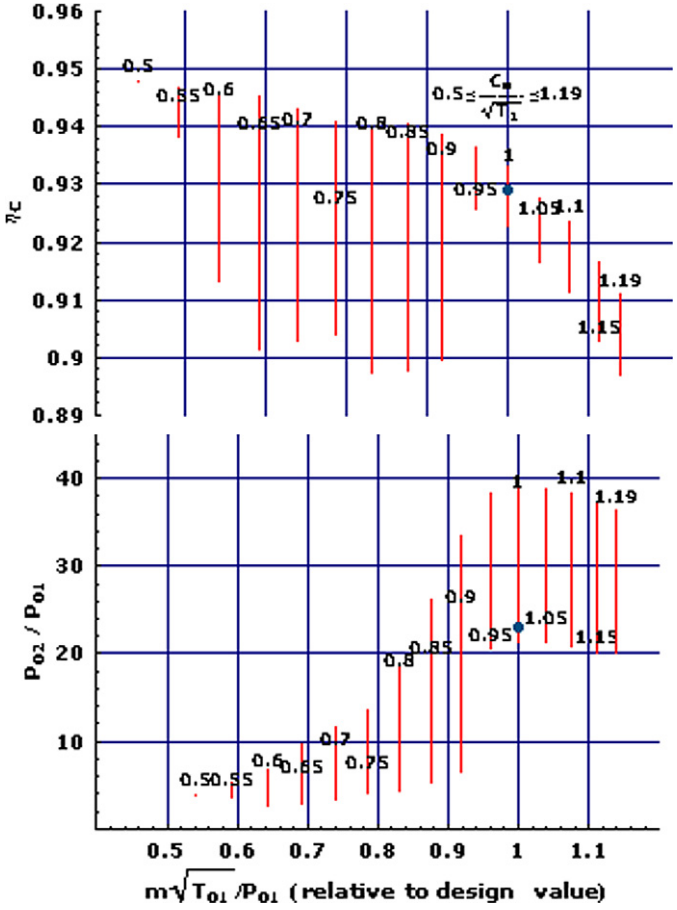

Fig. 7. Characteristic map of alternative compressor for different values of $\frac{C_a}{\sqrt{T_1}}$ (relative to design value).

nation pressure and temperature) does not change appreciably Fig. 7.

Efficiencies also show considerable improvement which is expectedly result of optimum rotational speed compatible with environmental elements (Figs. 6 and 7).

6. Conclusion

A method to introduce context-awareness into gas turbine engines was briefly presented in which linkage among components is replaced by coherent consistency under integrated management. Such configuration allows free access to components individually toward adaptation to environmental elements and user demands.

Based on this method an alternative to HPC of GE90-94B high by pass ratio turbofan engine was designed and modeled by computer in average-fidelity level. In this way, suitable methods to design and draw characteristic map of intended type were introduced. In addition, new dimensionless parameters were defined, which satisfy requirements of individual rotational speed for each stage in multi-stages axial flow compressors.

Summary of results indicates that this mechanism allows collecting optimum performance of compressor and advances its operation. Free access to each component allows adaptation of each stage to environmental elements and user demands whose outcome is such an adaptation for compressor entirely.

However, some points remain open:

- To detect flow separation in the stages, general methods usually used for preliminary design was adapted and implemented. Although these methods can preliminarily indicate effects of adaptation ability to user demands and environmental elements, but real behavior of flow is a complicated function of geometrical and aerothermodynamic properties of stage. As a result, to approach facts of flow condition in the stage when such ability is included, high-fidelity level analysis is necessary in which absolute characteristic of cascades are defined.
- In this study, conventional methods to detect flow separation and structural limitations were adapted to measure effects of rotational speed changes on those. However, stage characteristic along with rotational speed create a complex pattern to response to variation of rotational speed. As a result, detecting real response of stage to change of rotational speed needs a specific pattern in which influential parameters are considered together and accurate response of stage are wholly calculated.

References

[1] B. Aryana, Implementing DEA to create a novel type of compressor, 2007, http://babakaryana.tripod.com/Files/article2.pdf.
[2] H. Cohen, G.F.C. Rogers, H.I.H. Saravanamuttoo, Gas Turbine Theory, third ed., Longman Scientific & Technical, 1990, Chapter 5.
[3] M. Fennimore, T.D. Yuzvinsky, W.-Q. Han, M.S. Fuhrer, J. Cumings, A. Zettl, Nature 424 (2003) 408.
[4] P.G. Hill, C.R. Peterson, Mechanics and Thermodynamics of Propulsion, second ed., Addison-Wesley Publishing Company, 1992, Chapter 7.
[5] J.H. Horlock, Axial Flow Compressors, Butterworths, London, 1958.
[6] A.P. Malozemoff, J. Mannhart, D. Scalapino, High-temperature superconductors get to work, in: Physics Today, April 2005, pp. 41–45.
[7] T.P. Moran (Ed.), Special Issue on Context in Design, Human–Computer Interaction 9 (1994) 1–149.
[8] NASA-CR-174955 High Pressure Compressor (ICLS/10c) Compressor Performance Report Topical Report, Oct. 1983–Jul. 1985 (General Electric Co.) 120 p. X85-10387.
[9] J.A. Reed, M.G. Turner, A. Norris, J.P. Veres, Towards an automated full-turbofan engine numerical simulation, Prepared for the 16th International Symposium on Airbreathing Engines, sponsored by the International Society for Airbreathing Engines Cleveland, Ohio, August 31–September 5, 2003, National Aeronautics and Space Administration, Glenn Research Center.
[10] M.J. Zucrow, J.D. Hoffman, Gas Dynamics, John Wily & Sons, 1976, Chapter 8.
[11] http://www.wolfram.com.